X-616-68-293

PREPRINT

NASA TM X-63287

LARGE VELOCITY DISCONTINUITIES IN THE SOLAR WIND

L. F. BURLAGA

JUNE 1968

GSFC

GODDARD SPACE FLIGHT CENTER

GREENBELT, MARYLAND

LARGE VELOCITY DISCONTINUITIES IN THE SOLAR WIND

L. F. Burlaga*
Laboratory for Space Sciences
NASA-Goddard Space Flight Center
Greenbelt, Maryland

June 1968

*NAS-NRC Postdoctoral Reseach Associate

Abstract

In the course of 3000 hours observation of the interplanetary plasma, the plasma and magnetic field experiments on Explorer 34 have detected eleven discontinuous solar wind speed changes, not associated with shocks, of more than 60 km/sec in less than 3 min. These events, called uD's, may show a velocity change of either sign, but the plasma density and temperature are not found to change appreciably across them. Each speed discontinuity occurs simultaneously with a directional discontinuity in the magnetic field. High resolution magnetic field data show that sometimes the directional changes occur as rotational fans, and at other times they are erratic or occur within the time resolution of the magnetic field experiment, 2.6 sec. The flow direction of the solar wind changed at two of the eleven uD's. The quiet nature of the field and plasma on each side of these events gives the impression that they are stable. The existence of these uD's is shown to be consistent with the theory of the Helmholtz instability. In particular, the additional observation that the magnetic field direction change, ω , at a uD tends to be near 90° is consistent with the theory, for uD's with small ω may become unstable as they move from the sun.

I. Introduction

The existence of tangential discontinuities in the interplanetary medium has been suggested by several authors (see the review by Colburn and Sonett (1966)). A tangential discontinuity can be pictured as the boundary between two adjacent, rectangular, flux tubes (see Figure 1). The magnetic field and plasma parameters may differ in each tube, but the pressure normal to the boundary must be the same in both tubes. In principle, the tubes can move relative to one another along the surface between them (the glide plane). As the flux tubes are convected past the satellite, their relative motion can be observed as a discontinuity in the solar wind speed (Burlaga 1967a). Let us use the symbol uD to denote a solar wind speed discontinuity. Burlaga (1967_a) has shown that several types of tangential discontinuities do exist in the solar wind, and that small uD's (i.e., changes less than 15 km/sec which occur within 71 sec) are sometimes observed at directional discontinuities.

It is well known that in an ordinary fluid a velocity discontinuity (vortex sheet) is absolutely unstable. In a hydromagnetic fluid however, velocity discontinuities may be stable under certain conditions. Sen (1963) has presented two necessary conditions for stability in an incompressible, hydromagnetic fluid: 1) the streaming speed, V, must be less than $\sqrt{2}$ times the Alfven speed, V_A 2) the magnetic field direction must, in general, change by a sufficiently large amount at the

discontinuity. The effect of compressibility has also been studied by Sen (1964) who concludes that it is probably not significant when $V \approx V_A$.

The primary aim of this study was to determine whether large velocity discontinuities not associated with shocks exist in the solar wind, and if so, whether their existence is consistent with Sen's stability conditions. It is found that large uD's (i.e. changes in the solar wind speed which are >60 km/sec and occur in less than 3 min.) do exist. Such discontinuities occur when the magnetic field energy density exceeds the kinetic energy density and when $V_A \geq \Delta U$, where ΔU is the observed change in the solar wind speed. It is also found that magnetic field directional discontinuities always occur simultaneously with a large uD, and that the size of the directional discontinuity tends to be near 90°. No small ($\leq 45^\circ$) directional discontinuities were observed at the large uD's although Burlaga (1968b) has shown that, in general, small directional discontinuities were seen far more frequently than large ones during 1966. These observations are discussed in relation to Sen's stability criteria.

II. Instruments

The plasma and magnetic field data used for this study were obtained by Explorer 34, an earth-orbiting satellite with an apogee of 34 R_e. The data were obtained between May 30, 1967 and December 26, 1967 during which time the satellite spent $\approx$ 3000 hours in the interplanetary medium.

The plasma data were obtained with an instrument developed by Ogilvie et al., (1968). It consists of a velocity selector and an electrostatic analyzer which give proton and alpha particle spectra separately. The proton differential energy spectrum consists of 14 channels in the range 310 eV - 5100 eV., which form a geometric progression with a ratio 1.24:1 and have a full width $\frac{\Delta E}{E} \approx 5\%$. Since energy spectra are formed by counting for 2.6 sec. at each energy level, a typical 3-bar spectrum is obtained in 7.8 sec; successive proton spectra are obtained at 3 min. intervals.

The plasma distribution function f(v) for a given proton spectrum is represented by fitting the unfolded spectrum by a series of maxwellian arcs, as described by Burlaga and Ogilvie (1968) and Ogilvie et al., (1967). The fluid parameters - density n, mean speed u, and temperature T - are obtained by taking moments of f(v):

$$n = \int f(v)\, dv$$

$$u = \frac{1}{n} \int v\, f(v)\, dv$$

$$T = \frac{m}{nk} \left[\int v^2 f(v)\, dv - n u^2 \right]$$

With just a few exceptions, the plasma parameters presented in this paper were obtained from spectra containing 3 or 4 bars with counts greater than 2 standard deviations above the mean background counts. From such a spectrum, the mean speed can be determined with an error $<2\%$, but the density and to a greater extent the temperature are sensitive to the number of bars and the counting rate. To estimate the errors in the fluid parameters which are a consequence of the limited resolution of the instrument, a simulation program has been developed. This program computes the counts which the instrument would record in each energy channel if the plasma were maxwellian with parameters n', u', T', and it computes the fluid parameters would be measured (n'', u'', and T'') using the basic procedure described above. To test the accuracy of the actual measured parameters n, u, T, it is assumed that $n'=n$, $u'=u$ and $T'=T'$, and these parameters are introduced into the simulation program to compute n'', u'', and T''. If $n=n''$, $u=u''$, and $T=T''$, it is assumed that the measured parameters are correct. If $n\neq n''$, $u\neq u''$ and $T\neq T''$, the difference between the unprimed and double-primed quantities is taken as a measure of the errors in the measured fluid parameters due to instrumental resolution. As might be expected, these errors are largest when the density is low (giving low counts), when the mean speed is high (giving fewer bars and lower counts because of the wider spacing of

energy channels at higher energies) and when the temperature is low (giving few bars). It is found that the parameters are insensitive to the flow direction. The error in u is almost always <3%.

The plasma probe has coarse directional resolution, designed primarily for magnetosheath flow studies, which provides some information concerning interplanetary plasma flow direction. This information is obtained by recording the counts in each of 16, 22.5° sectors (see Figure 2) and transmitting the number of the sector containing the maximum number of counts. Figure 2 shows that radial solar wind flow with an abberation of 4° west is in a direction 3° east of the boundary between sectors 9 and 10. Clearly, radial flow produces the maximum number of counts in sector 9, while flow from > 3° W produces the maximum counts in sector 10. Thus, a change in the solar wind direction can be detected if it moves from a direction in sector 9 to a direction in sector 10, but the magnitude of the change cannot be determined.

The magnetic field data were obtained by Ness and Fairfield with a tri-axial, flux-gate magnetometer. The digitization error is $\pm .16\gamma$ and the components of the magnetic field are measured to an accuracy $\approx \pm .2\gamma$. Complete vector measurements of the magnetic field are determined at 2.56 intervals. Most of the magnetic field data below are 20.45 sec. averages computed by averaging eight successive measurements of each component of the magnetic field.

III. Observations

A. Definition and Identification of Large uD's

For convenience, let us use the symbol uD to denote a discontinuity in the mean solar wind speed, u. A large solar wind speed discontinuity is here defined as a change $\Delta u \geq 60$ km/sec. which occurs within 3 min., the time between successive spectra measured by the Explorer 34 plasma probe. The number 60 km/sec. is somewhat arbitrary; it was selected because it is a large change in the sense that few uD's have such a large Δu.

Large uD's are very notable on the mesoscale ($\approx \Delta$AU $\longleftrightarrow$ 4 days, see Burlaga (1968b)) and are clearly seen on the microscale ($\approx$ 1 hr. $\longleftrightarrow$ .01 AU). Figure 3 shows 4 uD's as seen on the microscale; this figure is discussed in detail below.

The large uD's which are analyzed below were selected as follows:

1) Solar wind speed measurements were examined in mesoscale plots (4 days data per page) and discontinuous ($\leq$ 3 min.) changes $\geq$50 km/sec were isolated for further study.

2) Individual measurements of the plasma parameters in a 30 min. interval centered on each uD were examined. If gaps in the plasma or magnetic field data occurred in the 30 min. interval, the uD was rejected.

3) The change in u, $\Delta u \equiv u_1 - u_2$, was computed for each uD, where u_1 is the speed measured 3-6 minutes before the arrival of the uD, and u_2 is the speed measured 3-6 minutes after the

uD. Only uD's with $\Delta u \geq 60$ km/sec were selected for further study.

4) UD's associated with the interplanetary shocks identified by Ogilvie and Burlaga (1968) were excluded.

The above procedure identified 11 large uD's (($\Delta u \geq 60$ km/sec) /(3 min.)) in 3000 hours of Explorer 34 interplanetary data during the period may 30, 1967 to December 26, 1967.

B. Plasma and Magnetic Field Parameters near uD's

The plasma and magnetic field parameters for 11 uD's are given in Table I. The tabulated plasma parameters are essentially means for the 9 minute intervals preceding and following each uD. The mean value for a 9 minute interval is not always the most appropriate one, so the numbers in Table I include a subjective judgement by the author which is based on simulation studies for these parameters as discussed in section II above, on the variation of the parameters before and after each uD, and on the author's general experience with the plasma probe data. However, the subjective changes are all within the errors quoted.

The errors quoted in Table I are based on the variation of the plasma parameters in the 9 minute intervals before and after each uD, and on the difference between the measured parameters and the parameters obtained by introducing the measurements into the simulation program, and are probably conservative.

Magnetic field data are given in Table I, rows 7-12, where B is the magnetic field intensity, ϕ is the solar ecliptic longitude ($\phi = 0^\circ$ if B is toward the sun, and $\phi > 0^\circ$ in the dusk meridian), and θ is the solar ecliptic latitude ($\theta > 0^\circ$ if B is directed north of the ecliptic plane). The data are essentially means for the 1 minute intervals which precede and follow each directional discontinuity (see below) associated with a uD. In the case of a rotation fan (see section IIIC), the numbers are based on data in the 1 minute intervals which precede and follow the fan. The **rms uncertainties which are quoted are larger than the measurement and digitization errors, so they represent real** time variations in the field before and after the uD's. It can be seen that these time variations are small ($\Delta B/B \approx 10\%$, $\Delta\theta \approx \Delta\phi \simeq 10^\circ$)

Several interesting results follow immediately from Table 1.

1) uD's with $\Delta u \geq 85$ km/sec. within 3 min. exist in the interplanetary medium (see Table 2, rows 1 and 2).

2) Large uD's usually occur when the solar wind speed is larger than average. For 9 of 11 uD's the wind speed exceeded 500 km/sec for 5 it exceeded 600 km/sec.

3) Large uD's usually occur when the temperature is $\gtrsim 10^5$ ^oK, when the density is $\lesssim 4/cm^3$ and when the magnetic field intensity is $\gtrsim 5\gamma$.

4) The density, temperature and magnetic field intensity do not change appreciably across a uD. This is seen in Table 2 which gives $n_1 - n_2$, $T_1 - T_2$, and $B_1 - B_2$. The density and temperature do not change at all within the errors quoted, and the change in B is less than $.5\gamma$ for 6 uD's. A small ($\simeq 1\gamma$ to 2γ), probably real, change in B was found for 5 uD's (2 increases and 3 decreases).

5) The magnetic field pressure, $B^2/8\pi$, dominated the plasma pressure, nkT, near all of the uD's. This is shown in rows 16 and 17 of Table 2 which give the ratio

$$\beta = \frac{nkT}{B^2/8\pi} = \frac{3.5\ n(cm^{-3})\ T(\circ 10^5)}{[B(\gamma)]^2} \qquad (1)$$

6) The pressure

$$P = \frac{B^2}{8\pi} + nkT = 10^{-12}\left[4(B(\gamma))^2 + 1.4\ T(\circ 10^5)\, n(cm^{-3})\right] \qquad (2)$$

is constant across each uD, within the experimental errors. The temperature used to compute p_1 and p_2 in Table 2 is the proton temperature. Strictly speaking, the electron temperature Te, should be included, but it is unknown. It would affect the pressure balance if T_{e_1} is much different from T_{e_2} and if max (T_{e_1}, T_{e_2}) is much greater than the proton temperature.

7) Each uD is associated with a discontinuity in the direction of the magnetic field. (For a discussion of directional discontinuities see Burlaga (1968b))

G. Directional Discontinuities Associated with uD's

Table I, rows 9 to 12, shows that each of the 11 large uD's is associated with a discontinuity in the direction of the interplanetary magnetic field. Figure 2, which shows 4 types of uD's, illustrates the general observation that the directional discontinuity and the discontinuity in mean speed are simultaneous within the time resolution of the plasma probe. The existence of a directional discontinuity indicates that the elemental flux tubes, which are in relative motion along the surface of a tangential discontinuity, are not parallel to one another.

The angular separation between the vectors $\underset{\sim}{B}_1$ and $\underset{\sim}{B}_2$ which preceed and follow a directional discontinuity is given by ω, where

$$\cos\omega = \underset{\sim}{B}_1 \cdot \underset{\sim}{B}_2 \,/\,(|\underset{\sim}{B}_1| \cdot |\underset{\sim}{B}_2|) \qquad (3)$$

$$\cos\omega = \cos\theta_1 \cos\theta_2 \cos(\phi_1 - \phi_2) + \sin\theta_1 \sin\theta_2 \qquad (4)$$

The angular changes, ω, were computed for each of the 11 uD's in Table I to an accuracy of $\pm 15^\circ$, using the parameters in rows 9 - 12 of that table; the results are recorded in Table 2, row 7. It is important to note that the smallest ω is 46°, the largest is 161°, and the mean value of ω is 93°. The values of ω are shown.

graphically in Figure 4c, which clearly shows the tendency to cluster about 90°, with 6 ω's $<90^{\circ}$ and 5 $\geq 90^{\circ}$. This distribution is quite suprising in that it is quite unlike the general distribution for directional discontinuities which was reported by Burlaga (1968b), viz. $dN/d\omega \propto \exp(-(\omega/75^{\circ})^2)$. There are at least 2 ways to explain this result:

1) The large uD's develop only at large directional discontinuities.

2) Large uD's are initially associated with both large and small directional discontinuities in the proportion implied by Burlaga's determination of $dN/d\omega$, but those with small ω become unstable and rapidly dissappear. We shall discuss this possibility in Section E below.

Another meaningful quantity associated with a directional discontinuity is the direction $\hat{n}$, where

$$\hat{n} = \underset{\sim}{B}_1 \times \underset{\sim}{B}_2 / (|\underset{\sim}{B}_1| \cdot |\underset{\sim}{B}_2|) \qquad (5)$$

This is the direction normal to the surface between two flux tubes separated by a tangential discontinuity. The vector $\hat{n}$ was computed for each of the 11 uD's. The solar ecliptic directions of these vectors are given in rows 8 and 9 of Table 2 and by a and b in Figure 4. The distribution of $\hat{n}$'s is similar to that found by Burlaga (1968b) for a much larger class of directional discontinuities.

When the magnetic field data for the large uD's are examined with the high time resolution data (2.6 sec), it is found that some of the associated directional "discontinuities" are actually structured. The top 2 curves in Figure 5 show how the magnetic field direction changed through the "discontinuities" at 0251 UT on day 216 and at 0917 UT on day 263. The dots are the high resolution measurements; the open circles are averages, each based on 8 successive measurements. Note that the magnetic field vector changes direction across the boundary between the adjacent flux tubes by rotating along a smooth curve. Siscoe et al., (1968) previously identified such rotation fans in the interplanetary medium, but they did not show that the fans may be associated with plasma discontinuities. Siscoe et al. showed that rotation fans tend to be planar. For a truly planar rotation fan there is a direction $\hat{n}'$ such that $\underset{\sim}{B}_i \cdot \hat{n}' = 0$, $i = 1, N$, where N is the number of vector measurements in the fan. In general, the vectors are not planar because of real and instrumental fluctuations, but we can calculate the normal to a plane about which the vectors are distributed by minimizing the quantity $\sum_i (\underset{\sim}{B}_i \cdot \hat{n}')^2$ subject to the constraint $(\hat{n}')^2 = 1$. For the fan at 0251 UT on day 216, this procedure gives a plane in the direction $\theta_n = 22^\circ$, $\phi_n = 54^\circ$. Table 2, rows 8 and 9 in column A, shows that within the experimental uncertainties, ($\Delta\theta \approx \Delta\phi \approx \pm 15^\circ$), this agrees with the direction of the glide plane normal computed from (5), viz. $\theta_N = 10^\circ$, $\phi_N = 55^\circ$. The average component of $\underset{\sim}{B}$ along $\hat{n}$ (i.e. normal to the glide plane) was found to be $(-.3 \pm .5)\gamma$.

A similar computation for the glide plane near 0917 UT on day 263 gives $\Theta_N = -56^\circ$, $\phi_N = 60^\circ$ which may be compared with $\Theta_n = -36^\circ$, $\phi_n = 33^\circ$, from column B in Table 2. The average component of $\underset{\sim}{B}$ normal to the plane determined by Θ_N, ϕ_N is $(1.5 \pm .6)\gamma$, which is $\approx 10\%$ of the total field.

The field does not always change through a directional discontinuity by means of a rotation fan. Figure 5 shows that the field moved very erratically through the directional discontinuity associated with the uD at 0106 UT on day 340. However, Figure 3 a shows that the field direction was fluctuating appreciably at high frequencies throughout the period near this uD. There are other uD's at which the change in magnetic field direction occurs within 2.6 sec. so that no rotation of any kind can be measured for these uD's (e.g. the uD at 1542 UT on day 314).

D. Change in Flow Direction at a uD

As discussed in Section II the plasma probe on Explorer 34 can detect changes in the solar wind direction under certain conditions. In particular, one can determine whether the maximum flow is into sector 9 or sector 10, as illustrated in Figure 2.

Figure 6 shows the measured flow direction in an hour interval centered about the uD at 0105 UT on day 340. Before the discontinuity arrived, the flow was into sector 10 (see Figure 1). Immediately after the uD, the flow was into sector 9, and it varied between sectors 9 and 10 for 30 minutes after the uD. Thus, it is established that a change in flow direction can occur at a uD. Since the uD was accompanied by a directional

discontinuity, we also have the result that the solar wind direction may change at a discontinuity in the magnetic field direction. Figure 6 also shows direction data for another uD, at 0900 UT on day 340, which gives the same results. A change in flow direction is expected in general if a uD is produced by gliding flux tubes (see Burlaga 1968a, Figure 6).

E. Stability of a uD.

We have observed that large uD's do exist in the interplanetary medium and that the magnetic field near them is not unusually disturbed (see the illustrative examples in Figure 3 and the uncertainties in B, θ, and ϕ in Table 1), suggesting that the uD's are stable. It was also shown that all of the uD's were observed simultaneously with directional discontinuities in the interplanetary magnetic field and that these discontinuities were usually large, with the direction changes tending to be near 90°. Let us now examine these observations in terms of the Helmholtz instability.

Sen (1963) has determined two necessary conditions for stability in an incompressible hydromagnetic fluid, viz.

$$\left(B_1^2 + B_2^2\right)/4\pi \geq \frac{\rho_1 \rho_2 V^2}{(\rho_1 + \rho_2)} \qquad (6)$$

and

$$\left(\underset{\sim}{B}_1 \times \underset{\sim}{B}_2\right)^2 \geq \frac{4\pi \rho_1 \rho_2 V^2}{(\rho_1 + \rho_2)} \left[\left(\underset{\sim}{B}_1^{\perp}\right)^2 + \left(\underset{\sim}{B}_2^{\perp}\right)^2 \right] \qquad (7)$$

where ρ is the mass-density, V is the relative speed between two streamers, and $\underset{\sim}{B}^{\perp}$ is the component of $\underset{\sim}{B}$ perpendicular to the relative velocity $\underset{\sim}{V}$. When $B_1 \approx B_2$ and $\rho_1 \approx \rho_2$, as we have observed for the 11 large uD's, (6) and (7) reduce to

$$\sqrt{2}\, V_A > V \qquad (8)$$

and

$$\sin^2\omega \geq \frac{1}{2}\left(\frac{V}{V_A}\right)^2 \left[\frac{(B_1^{\perp})^2 + (B_2^{\perp})^2}{B^2}\right] \qquad (9)$$

where V_A is the Alfven speed,

$$V_A\,(km/sec) = \frac{21.8\ B(\gamma)}{\sqrt{n\,(cm^{-3})}} \qquad (10)$$

Equations (8) and (9) are equivalent to those given by Landau and Lifshitz (1960) for stability in an incompressible fluid.

Let us assume for the moment that the interplanetary medium can be described as an incompressible fluid, and ask whether the observations of large uD's are consistent with (8) and (9). Equation (9) shows that a uD is absolutely unstable if the magnetic field direction does not change across the discontinuity (unless the field happens to be parallel to V). In other words, a directional discontinuity must accompany a uD if $\underset{\sim}{B}$ is not parallel to $\underset{\sim}{V}$. The observations are consistent with this result. The LHS of (9) is maximum when the direction of $\underset{\sim}{B}$ changes by $\omega = 90^{\circ}$ at a uD. To

determine the RHS of (9) it is necessary to know $\underset{\sim}{V}$, but this has not been measured. When ω is near 0° or 180° and $\underset{\sim}{B}$ is nearly perpendicular to $\underset{\sim}{V}$, the RHS of (9) is approximately $V^2/(2V_A^2)$, and stability is possible only for $V \ll V_A$. When ω is near 0° or 180° and $\underset{\sim}{B}$ is nearly parallel to $\underset{\sim}{V}$, the RHS of (9) is on the order of $(\frac{\Phi}{2})^2 V^2/(2V_A^2)$, and stability is possible only if $V^2 < 8V_A^2$. When $\omega = 90^{\circ}$, the RHS of (9) is $V^2/(2V_A^2)$ for all $\underset{\sim}{B}$. Thus, in general, discontinuities with ω near 90° are more likely to be stable than those with small ω. The observations that ω tends to be near 90°, and that there are no small ω's at uD's, even though Burlaga (1968b) has shown that in general directional discontinuities with small ω's are most probable, may be explained by (9). For example, suppose that near the sun there are uD's with $V \ll V_A$; then (9) may be satisfied for uD's with both large and small directional discontinuities. Now $\rho \alpha r^{-2}$ and $B \alpha r^{-2}$, where r is the distance from the sun, so $V_A \alpha r^{-1}$. Thus, for a given constant ω and V, the uD will ultimately be convected to an r where (9) is not satisfied, as Parker (1963) has noted, and the uD's with small ω will become unstable before those with $\omega \approx 90^{\circ}$, as shown by (9).

The stability condition (8), i.e. $V < \sqrt{2}V_A$, must be satisfied regardless of the value of ω. We cannot test this condition directly since we measure only Δu, the radial component of $\underset{\sim}{V}$ (see Burlaga, 1968a, equation (6)). Table 2, rows 10, 11, 13, and 14 shows that all of the 11 large uD's satisfy (8) if $V < 1.1\ \Delta u$, 9 satisfy (8) if $V < 1.4\ \Delta u$, and 4 satisfy (8) if $V < 2\Delta u$. Thus, the existence of the large uD's in Table 1 is consistent with (8) is $V \approx \Delta u$. Since $\Delta u \leq V$, and since we have

selected only the largest Δu's, it is indeed probable that $V \approx \Delta u$ for the uD's in Table 1.

The preceding discussion shows that the characteristics of large uD's can be understood in terms of the theory of the Helmholtz instability in an incompressible medium. Strictly speaking, the assumption of incompressibility is not valid, for it implies that the speed of sound V_s, is much greater than the Alfven speed, which is not even approximately true for the uD's in Table 2 (see rows 10, 12, 13, and 15). Thus, we must determine whether compressibility plays a significant physical role in the Helmholtz instability. Parker (1963) has studied the problem for the case $\underset{\sim}{B_1} = \underset{\sim}{B_2}$ and $\underset{\sim}{B}$ parallel to $\underset{\sim}{V}$; he finds two necessary conditions for instability;

$$V^2 < 2 V_s^2 \tag{11}$$

and

$$V_A^2 < V_s^2 \tag{12}$$

where

$$V_s = \sqrt{\frac{\gamma P}{\rho}} = 37 \sqrt{T(^\circ 10^5)} \quad (km/sec) \tag{13}$$

Table 2 shows that the first of these conditions is not satisfied if $V \approx \Delta u$, and the second condition is not satisfied in any case.

Therefore, stability is not ruled out. The same problem, $\underset{\sim}{B}_1 = \underset{\sim}{B}_2$ and $\underset{\sim}{B}$ parallel to $\underset{\sim}{V}$, was treated by Sen (1964) who showed that the compressibility has little effect when $V \ll V_A$, and that is has a stabilizing effect for $V \gg V_A$. Thus the effect of compressibility strengthens our interpretation. The more general case $\underset{\sim}{B}_1 \neq \underset{\sim}{B}_2$ and $\underset{\sim}{B}$ not parallel to $\underset{\sim}{V}$ was also studied by Sen (1964) who concluded that the compressibility will probably have a destabilizing effect if $V \ll \sqrt{V_A^2 + V_s^2}$ and a stabilizing effect if $V \gg \sqrt{V_A^2 + V_s^2}$. Since $V \lesssim V_A$ and $V_S < V_A$ for our uD's, we expect the effect of compressibility to be small. Since compressibility is expected to have no large physical effect, equations (8) and (9) may give reasonable results.

IV. SUMMARY

This paper discusses large, discontinuous changes in the solar wind speed (changes not associated with interplanetary shocks) which were observed in 3000 hours of data obtained between May 30, 1967 and December 26, 1967. The results are as follows:

1) The solar wind speed may change by more than 85 km/sec. in less than 3 minutes as it is convected past the earth orbiting satellite. This corresponds to a gradient at least of the order of (85 km/sec)/(10^5km). Eleven solar wind speed discontinuities with $\Delta u \geq 60$ km/sec within 3 min. were observed in 3000 hours of data. Since several doubtful cases were ruled out for instrumental reasons, eleven is a lower limit on the number of large uD's which actually existed. Seven of these showed an increase in u and 4 showed a decrease in u.

2) Most of the uD's occurred when u, T and B were high and n low. The pressure was constant across each of the uD's within the errors. A small increase (1γ to 2γ) in B was observed for 5 uD's (2 increased and 3 decreased).

3) Each uD was associated with a directional discontinuity in the magnetic field $\underset{\sim}{B}$. The high resolution magnetic field data show that a.) in some cases the field changes rotating in a plane whose normal is in the direction $\underset{\sim}{B}_1 \times \underset{\sim}{B}_2$. b.) in other cases the field changes direction across the discontinuity by moving very erratically, and c.) sometimes the direction

change is complete in 2.6 s and this cannot be studied in detail. The changes in the magnetic field direction at uD's ranged from 46° to 161° and tended to be near 90°; the average ω was 93°. The changes are thus much larger than those normally observed at directional discontinuities. The vectors $\underset{\sim}{B}_1 \times \underset{\sim}{B}_2$ for the directional discontinuities at the large uD's were distributed as usual for directional discontinuities, namely, perpendicular to the spiral direction and out of the ecliptic plane.

4) The flow direction was observed to change at 2 large uD's. Thus, the flow direction may change at a directional discontinuity.

5) The existence of the large uD's is consistent with the theory of the Helmholtz instability. It is suggested that large uD's with small ω were formed, but disintegrated by means of the Helmholtz instability, leaving only uD's with ω near 90°.

ACKNOWLEDGEMENTS

The plasma data used in this study were provided by Drs. K. W. Ogilvie and T. W. Wilkerson; the magnetic field data were provided by Drs. N. F. Ness and D. H. Fairfield. These experimenters also contributed useful comments and suggestions concerning the manuscript. Dr. H. E. Taylor gave me his minimization program and also contributed many helpful suggestions.

REFERENCES

Burlaga, L. F.: 1968a, "Micro-scale Structures in the Interplanetary Medium," Solar Physics, 4, 134 - 159.

Burlaga, L. F.: 1968b, "Directional Discontinuities in the Interplanetary Magnetic Field," NASA-GSFC Preprint X-616-68-224 , June.

Burlaga, L. F., and Ogilvie, K. W.: 1968; "Observations of the Magnetosheath-Solar Wind Boundary," to Appear in J. Geophys. Res.

Colburn, D. S. and Sonett, C. P.: 1966, "Discontinuities in the Solar Wind," Space Sci. Rev. 5, 439 - 506.

Landau, L. D. and Lifshitz, E.M.: 1960, "Electrodynamics of Continuous Media." Pergamon Press, New York.

Ogilvie, K. W. and Burlaga, L. F.: "Interplanetary Shocks and the Plasma Flow behind them," to be published.

Ogilvie, K. W., Burlaga, L. F., and Richardson, H., 1967, "Analysis of Plasma Measurements on IMP-F," NASA-GSFC Report X-612-67-543, December.

Ogilvie, K. W., McIlwraith, N., and Wilkerson, T. D.: 1968, "A Mass-Energy Analyzer for Space Plasmas," Rev. Sci. Instr., In press.

Parker, E. N.: 1963, "Dynamical Properties of Stellar Coronas and Stellar Winds, III. The Dynamics Coronal Streamers," Ap. J. 139, 690 - 709.

Sen, A. K. : 1963, "Stability of Hydromagnetic Kelvin-Helmholtz Discontinuity," Phys. Fluids, 6, 1154 - 1163.

Sen, A. K.: 1964 "Effect of Compressibility on Kelvin-Helmholtz Instability in a Plasma," Physics of Fluids, 7, 1293 - 1163.

Siscoe, G. L., Davis, L., Jr. Coleman, P. J., Jr., Smith, E.J. and Jones, D. E.: 1968, "Power Spectra and Discontinuities in the Interplanetary Magnetic Field: Mariner 4", J. Geophys. Res., 73, 61 - 82.

FIGURES

Figure 1. A schematic illustration which describes a tangential discontinuity in terms of two hypothetical, rectangular, magnetic flux tubes. The figure shows the special case when the flux tubes are mutually perpendicular and inclined at an angle θ with respect to the ecliptic plane. The tubes are shown separated by a rotation fan.

Figure 2. The upper diagram shows the arrangement of the detector relative to the sun sensor in the satellite. The sensitive cone of the detector is 2° wide. The rotation direction shown here is that which is seen by an observer north of the ecliptic plane. The on-board computer stores the counts which are recorded as the sensitive cone moves through each of these 22.5° sectors; the counts are recorded in the sequence given by the numbering of the sectors. The number of the sector with the maximum number of counts is transmitted, and indicates the flow direction.

Figure 3. This shows the temperature, mean speed, density, magnetic field intensity, and magnetic field direction for each of 4 uD's. The top left sh ws a case in which high frequency fluctuations in the magnetic field were present (only the envelope of these fluctuations is shon). Six uD's in Table 2 (E, F, G, H, I and K) are of this type. The top right shows a uD with 2 directional

discontinuities occuring within the plasma resolution time; two uD's (J and D) are of this type. No fluctuations were observed at 4 uD's (B, C, D, and J), as illustrated by the uD on the bottom right of this figure. Both uD's in the lower half of this figure contain rotation fans at the directional discontinuities.

Figure 4. Figure 4a shows the solar ecliptic latitude of the vectors $\underset{\sim}{B}_1 \times \underset{\sim}{B}_2$ for each of the larger uD's in Table 1. The Figure 4b shows the corresponding longitudes. Note that the vectors tend to be directed away from the ecliptic plane and normal to the spiral field direction, as is characteristic of directional discontinuities. Figure 4c shows the values of ω for the directional discontinuities at the large uD's. Note the absence of small ω's and the tendency to cluster near 90°.

Figure 5. The top two curves are rotation fans associated with large uD's. The points were measured at 2.5 sec intervals, and the open circles are 20 second averages. The magnetic field vector changed direction by a rotation in a plane. The bottom curves shows a case for which the magnetic field changed direction across a directional discontinuity by moving very erratically.

Figure 6. This shows that the solar wind may change direction at a uD. The points indicate flow into sector 9 or 10 (see Figure 2). The points are at 3 minute intervals, and the dashed line indicates the time of the uD.

Table 1. The plasma and magnetic field parameters for 11 large uD's.

Table 2. Calculated quantities for 11 large uD's. The quantities p, ω, ϕ_n, θ_n, V_A, v_s and β were calculated from equations (2), (4), (5), (5), (10), (13) and (1), respectively.

TABLE 1

	A	B	C	D	E	F	G	H	I	J	K	
DAY	216	263	263	272	303	314	314	321	340	340	340	
HOUR	0251	0917	2221	2000	1955	1542	2205	0551	0106	0900	1137	
u_1 (km/sec)	400±7	485±20	777±12	700±8	481±20	457±4	395±20	450±25	600±7	633±10	604±9	1
u_2 (km/sec)	336±2	590±6	869±4	615±5	398±10	522±14	504±20	535±5	540±10	572±6	545±5	2
n_1 (cm^{-3})	2.3±1.5	1.6±.3	2.5±.3	1.8±.2	1.4±1.0	1.4±.4	2.0±1.0	2.0±.4	4.0±1.2	3.6±.6	4.3±.5	3
n_2 (cm^{-3})	1.5±.3	4±2	2.0±1.0	1.9±.2	1.0±.8	1.9±.2	2.0±1.0	2.0±.5	2.5±.5	3.5±.6	3.0±1.0	4
T_1 (10^5 °K)	.8±.5	1.5±1.0	2.7±1.5	3.0±.5	1.5±1.0	2±1	4±3	1.5±.4	2.5±.5	4.3±1.5	2.7±.4	5
T_2 (10^5 °K)	1±3	.7±.3	3.3±1.0	4.3±1.0	1.0±.8	2±1	8±4	1.5±.5	2±1	3.8±10	2.5±1.3	6
B_1 (γ)	4.8±.5	11.7±.2	10.8±.5	7.2±.2	3.8±.4	4.6±.2	5.8±.2	5.4±.2	7.8±.2	8.6±.5	9.6±.2	7
B_2 (γ)	4.5±.2	11.2±.2	12.3±.6	7.2±.2	4.9±.3	5.2±.1	5.9±.3	5.7±.3	7.6±.2	7.4±.6	7.7±.5	8
ϕ_1 °	151±10	270±4	317±10	351±5	194±10	338±10	72±5	320±10	92±10	141±5	264±10	9
ϕ_2 °	312±5	149±2	130±5	107±3	333±5	100±5	113±3	213±15	341±15	330±4	322±10	10
θ_1 °	29±10	-37±6	12±10	-65±10	29±8	62±10	34±5	15±15	29±4	-40±5	50±10	11
θ_2 °	-20±4	-31±3	(49±3)	-60±5	63±5	50±4	-20±3	47±6	56±15	15±6	-15±5	12

TABLE 2

	A	B	C	D	E	F	G	H	I	J	K	
DAY (1 Jan=1)	216	263	263	272	303	314	314	321	340	340	340	
HOUR	0251	0915	2221	2000	1955	1542	2205	0551	0106	0900	1137	
$(u_1 - u_2)$ (km/S)	64±7	-105±20	-92±13	85±9	83±22	-65±15	-109±28	-85±25	60±12	61±12	59±9	1
$(n_1 - n_2)(cm^{-3})$	.8±1.5	-2.4±2.0	.5±1.0	-.1±.3	.4±1.3	-.5±.4	0±1.4	0±.6	1.5±1.3	.1±.8	1.3±1.1	2
$(T_1 - T_2)(10^5 {}^oK)$	.2±.6	.8±1.0	.6±1.8	-1.3±1.1	.5±1.3	0±1	4±5	0±.6	.5±1.1	.5±1.1	.2± 1.4	3
$(B_1 - B_2)$ (γ)	.3±.5	.5±.3	-1.5±.8	0±.3	-1.1±.5	-.6±.2	-.1±.4	-.3±.4	.2±.3	1.2±.8	1.9±.5	4
$P_1 (10^{10} dynes/cm^2)$	1.2±1.1	5.8±4.0	5.6±3.3	2.8±1.1	.9±1.0	1.2±.7	2.5±2.3	1.6±.5	3.8±1.5	5.0±2.0	5.3±1.2	5
$P_2 (10^{10} dynes/cm^2)$	1.0±.4	5.4±3.6	7.0±4.2	3.2±.8	1.2±1.3	1.6±.8	2.5±1.8	1.7±1.0	3.0±1.5	4.0±1.3	3.4±2.0	6
ω^o	161	93	118	46	82	59	66	90	77	154	82	7
$\phi_N{}^o$	10	33	226	45	95	212	189	243	19	244	42	8
$\theta_N{}^o$	55	-36	5	15	15	17	34	-39	-28	-15	32	9
v_{A_1}	69±46	202±15	149±12	117±63	70±60	84±24	89±45	83±17	85±25	99±18	101±10	10
$\|\Delta u\|$	64±7	105±20	92±13	85±9	83±22	65±15	109±28	85±16	60±12	61±12	59± 9	11
v_S	33±10	45±14	61±17	64±17	45±16	52±13	74±27	45±6	58±6	77±13	61±12	12
v_{A_2}	80±16	122±61	189±37	114±11	107±32	82±8	91±46	88±23	105±21	86±17	97±12	13
$\|\Delta u\|$	64±7	105±20	92±13	85±9	83±22	65±15	109±28	85±16	60±12	61±12	59±9	14
v_S	37±6	31±7	67±10	77±19	37±15	52±13	109±28	45±13	52±13	72±15	59±15	15
β_1	.27	.06	.20	.36	.50	.47	.82	.35	.57	.72	.43	16
β_2	.26	.08	.15	.54	.14	.48	1.5	.31	.30	.84	.44	17

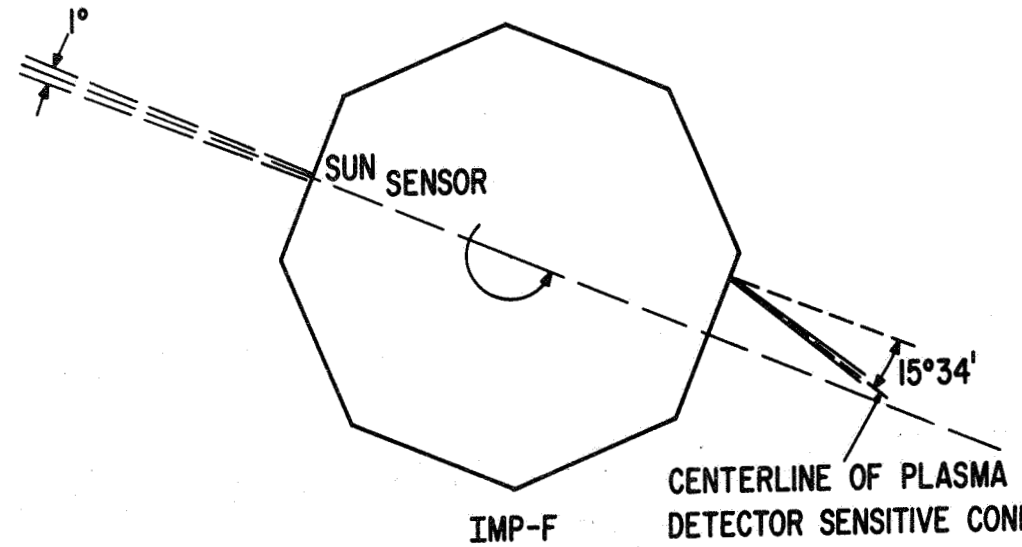
1°
SUN SENSOR
15°34'
CENTERLINE OF PLASMA
DETECTOR SENSITIVE CONE
IMP-F

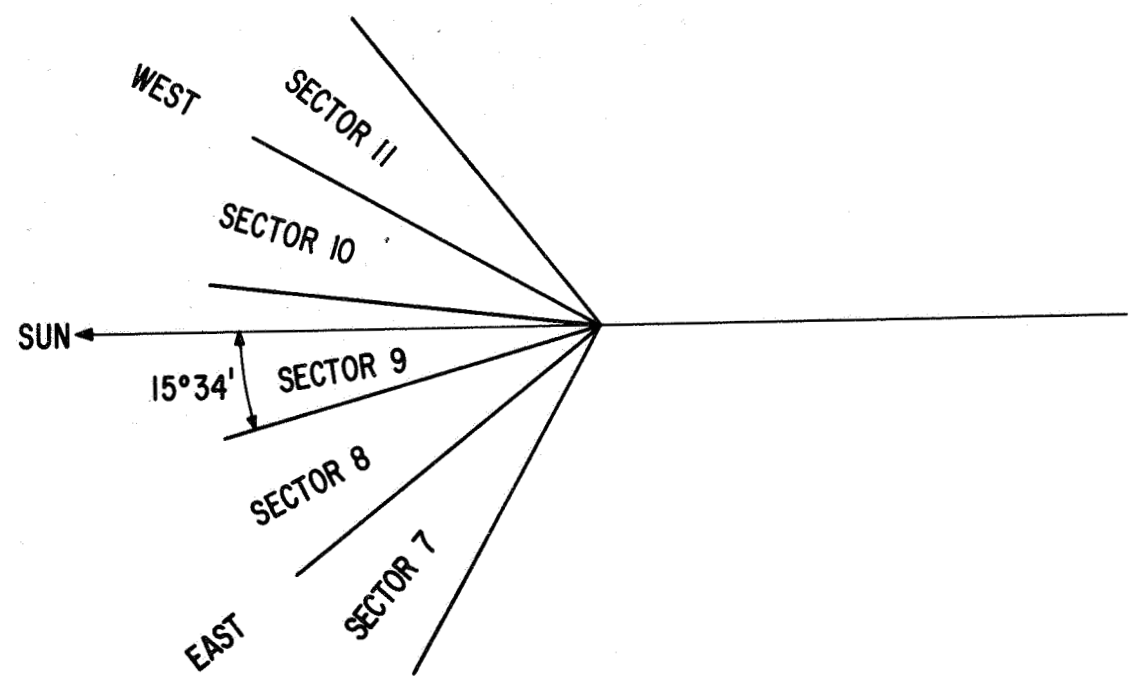
WEST
SECTOR 11
SECTOR 10
SUN
15°34'
SECTOR 9
SECTOR 8
SECTOR 7
EAST

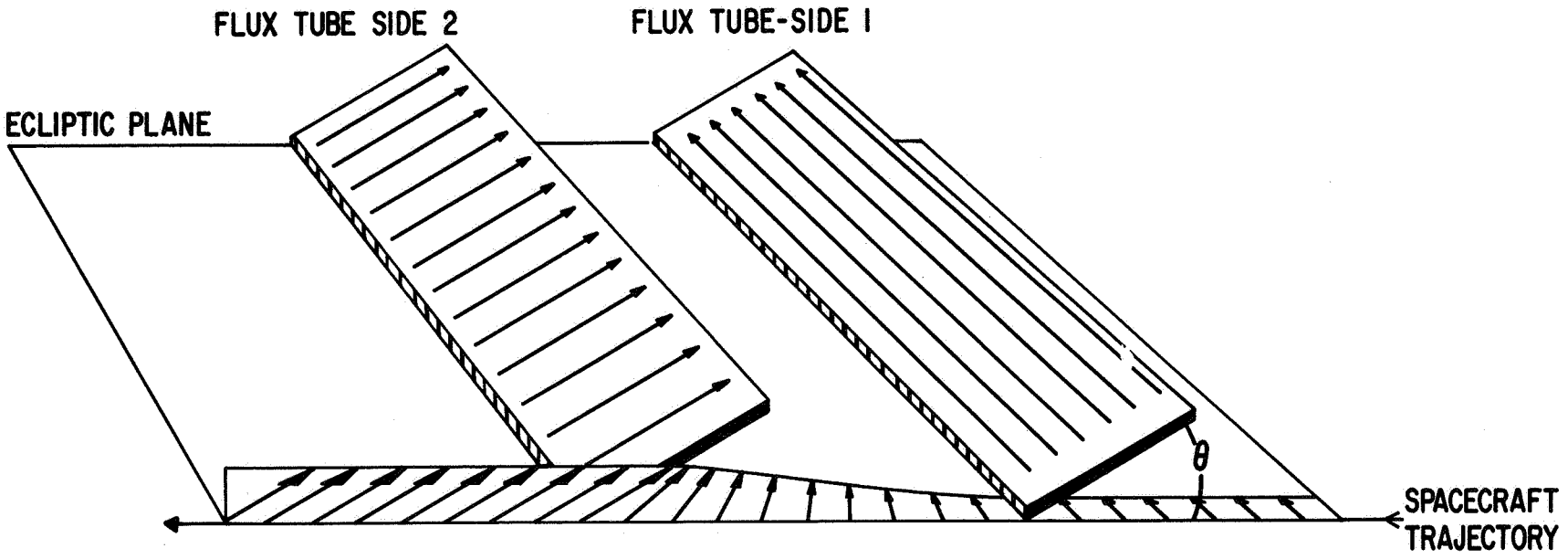

TANGENTIAL DISCONTINUITY

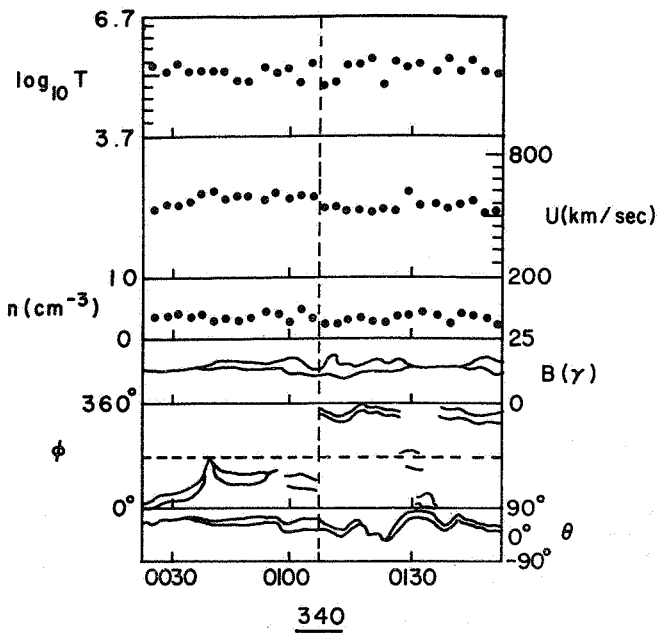

340

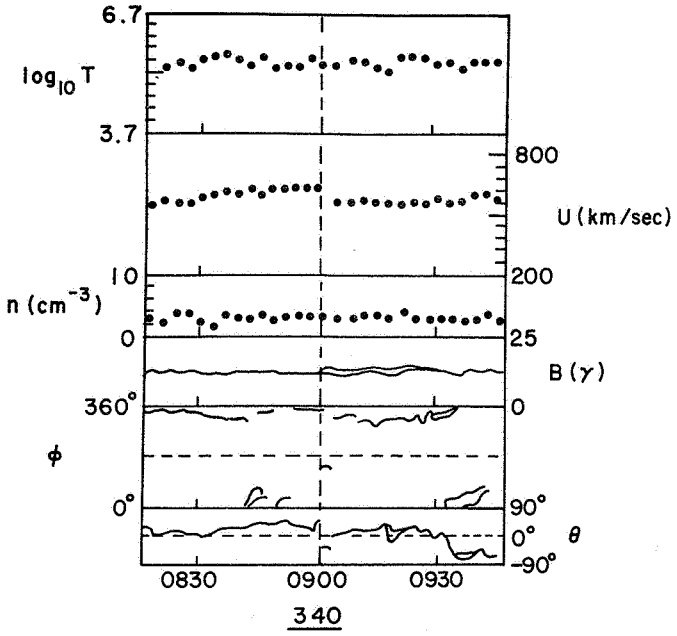

340

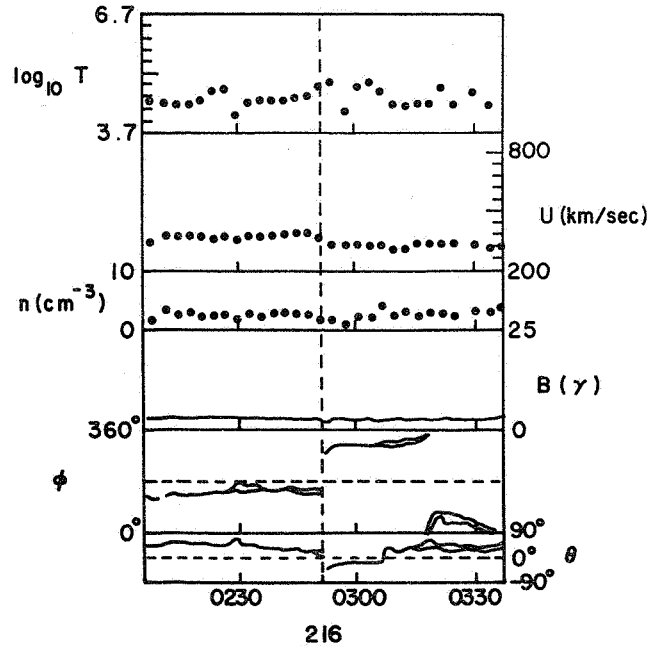

216

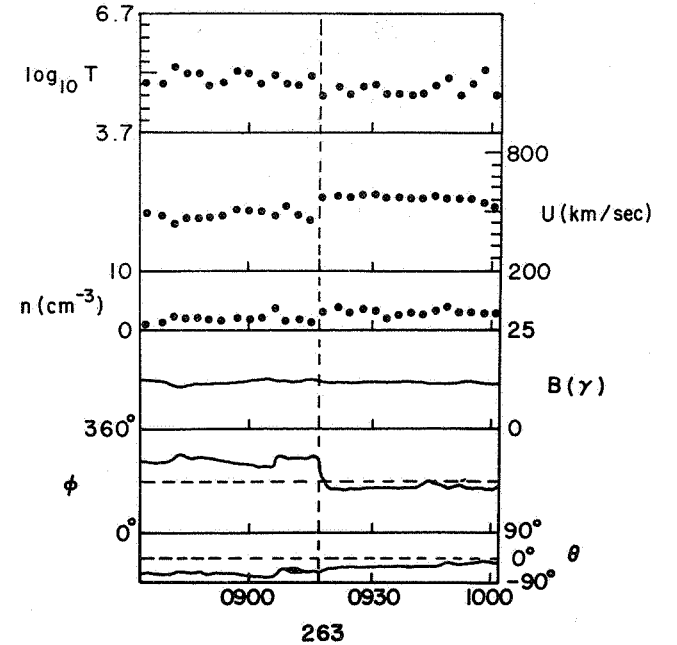

263

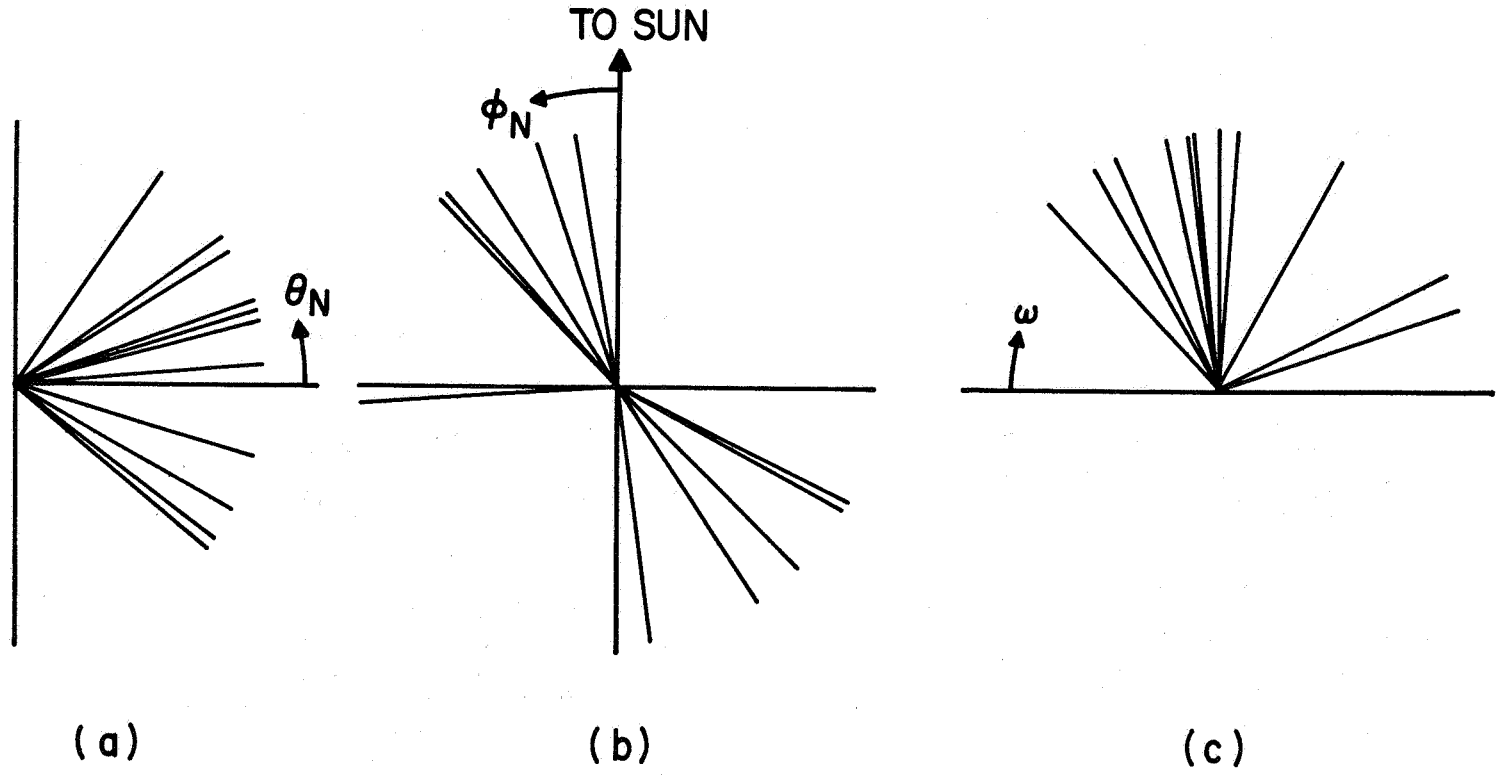
TO SUN
ϕ_N
θ_N
ω
(a)
(b)
(c)

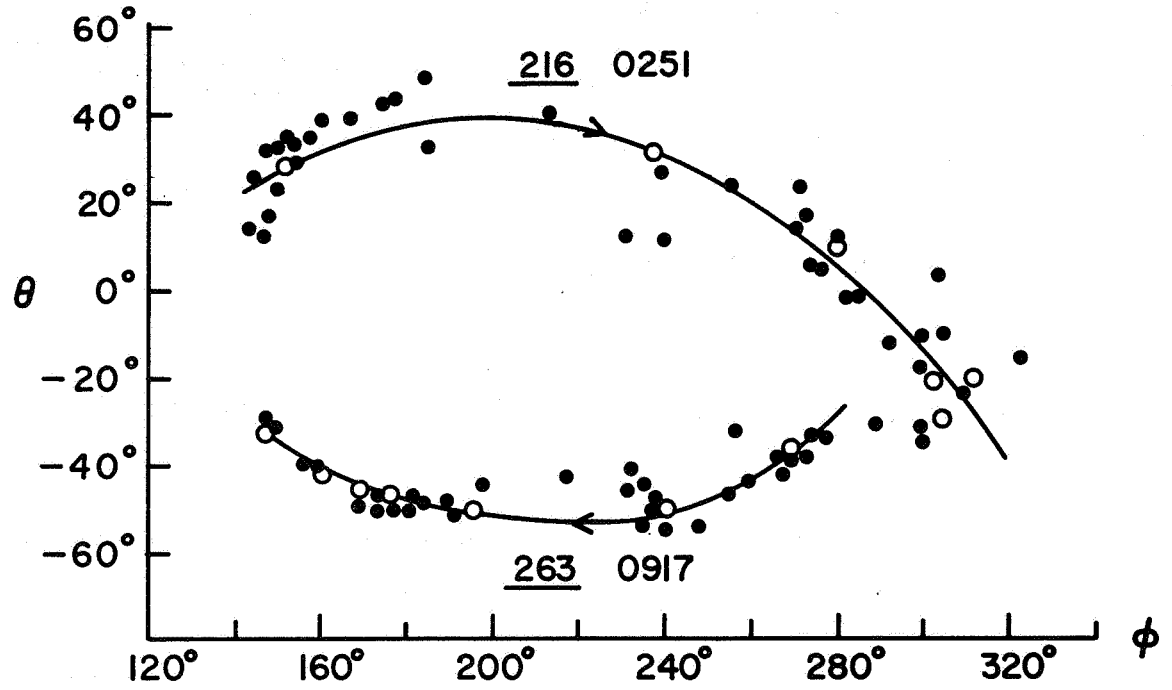
60°
40°
20°
θ 0°
−20°
−40°
−60°
216 0251
263 0917
120°
160°
200°
240°
280°
320°
φ

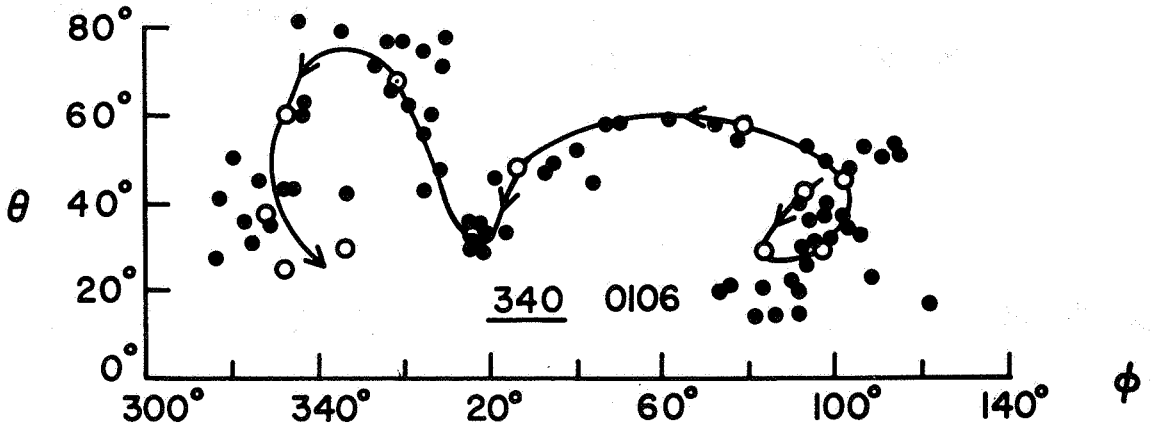
80°
60°
θ 40°
20°
0°
340 0106
300°
340°
20°
60°
100°
140°
φ

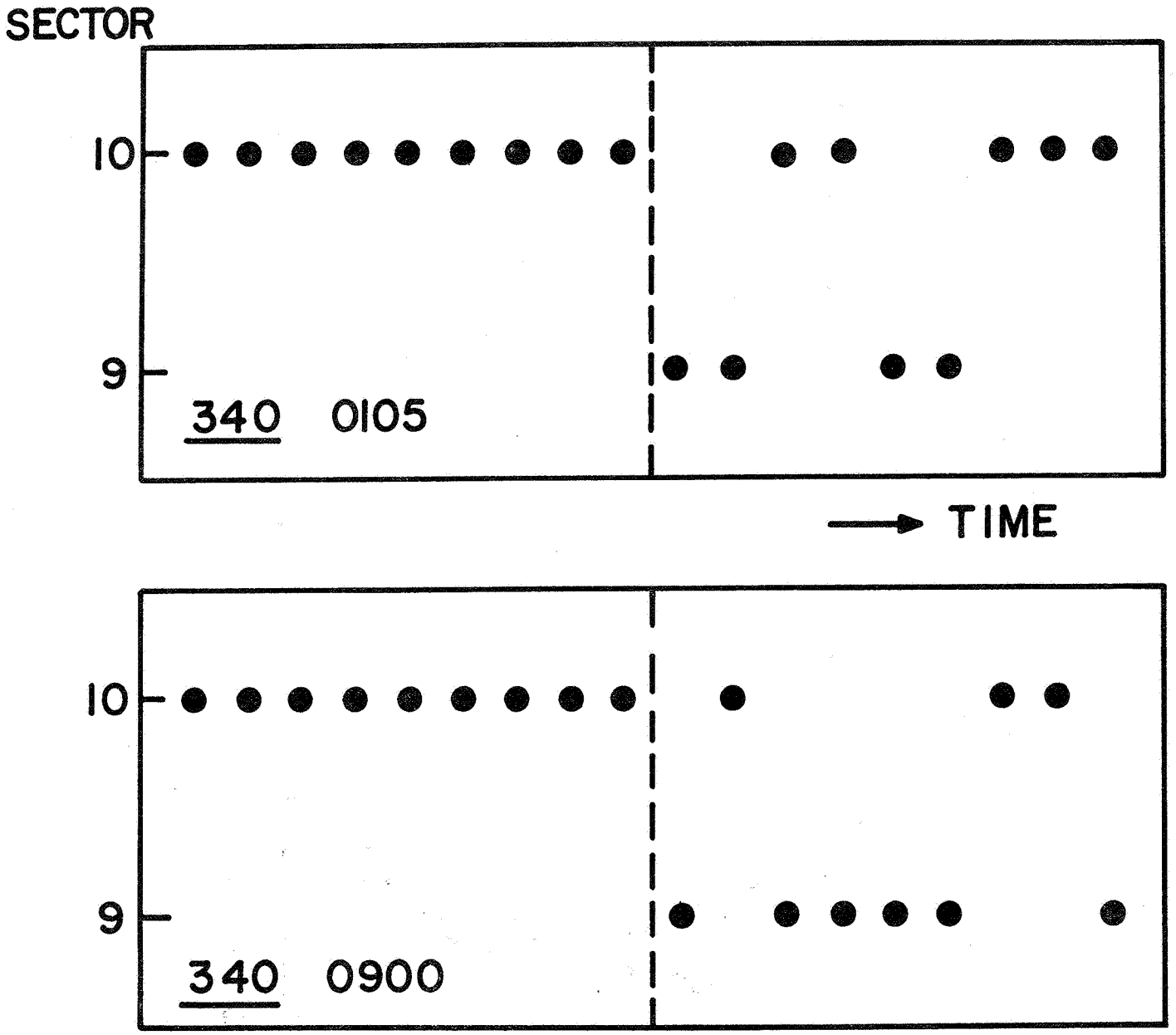
SECTOR
10
9
340 0105
TIME
10
9
340 0900